

Experimental Investigation of Laser Power Effect on Growth Rate of Intermetallic Compound in Al/Cu Bimetal Produced by Laser Cladding Method

M. A. Amani Tehrani

Department of Mechanical and Aerospace Engineering,
Science and Research Branch, Islamic Azad University, Tehran, Iran
E-mail: m.amni_amani@yahoo.com

S. Rahmati* & M. Najafi

Department of Mechanical and Aerospace Engineering,
Science and Research Branch, Islamic Azad University, Tehran, Iran
E-mail: rahmati@rapidtoolpart.com,
*Corresponding author

Received: 14 December 2015, Revised: 24 February 2016, Accepted: 17 April 2016

Abstract: The aim of this project is to fabricate an aluminium-copper bimetal through the fusion method and examine its performance. An aluminium-copper-aluminium bimetal was built by the laser cladding method. The laser power as well as the annealing time effects on its interfacial properties of the bonding's formed through the laser cladding were investigated. To fabricate the multilayer bimetal, the laser beam characteristic including the beam radius, and Transverse Electromagnetic Mode (TEM), and focusing conditions were considered in a heat source model. The model was, next, integrated within ANSYS package to predict the temperature distribution and clad bead profile during the laser cladding of the pre-placed copper powder layer on the aluminium substrate. After preparation of the samples, the intermetallic compounds formed at the joints were explored through the Scanning Electron Microscopy (SEM) and Energy Dispersive Spectroscopy (EDS) processes. Based on the experimental results, a laser power increase from 1100 W to 1150 W increased the intermetallic compound width, while an increase of 1150 W to 1200 W does not have much effect on the width. Also, increasing the annealing time results, increases the intermetallic compound thickness. In addition, based on experimental results obtained, four specimens are detected at the bimetal interface, one of which has 73.4 % copper and 26.1 % aluminium. The results also indicate that, with increasing both the laser power and annealing time, the electrical resistance of the samples decreases.

Keywords: Aluminium, Copper, Intermetallic growth, Laser cladding.

Reference: Amani Tehrani, M. A., Rahmati, S., Najafi, M., 'Laser power effect on growth rate of intermetallic compound in Al/Cu bimetal produced by laser cladding method', Int J of Advanced Design and Manufacturing Technology, Vol. 9/No. 1, 2016, pp. 21–32.

Biographical notes: **M .A. Amani Tehrani** received his M.sc in Mechanical Engineering from University of IAU Science and Research Branch, Tehran, Iran. **S. Rahmati** received his PhD in Advanced Manufacturing Technology from University of Nottingham, England in 1999. He has also received his MSc and BSc from Loughborough University in UK and Ottawa University in Canada respectively. He is currently Associate Professor of Mechanical engineering at the University of IAU, Science and research Branch, Tehran, Iran. His current research interest includes Additive Manufacturing, Medical Rapid prototyping, Advanced Manufacturing Process and Rapid Tooling. **M. Najafi** is Associate Professor of Mechanical engineering at the IAU Science and Research Branch, Tehran, Iran.

1 INTRODUCTION

Nowadays, a growing need is felt for the use of materials with special capabilities and characteristics, including high mechanical, electrical and, thermal properties. A single material by itself cannot satisfy these requirements. Therefore, the use of multilayer plates has been on the rise. These different metal layers including similar and dissimilar layers, will complement each other with respect to the mechanical, physical, chemical properties as well as economic benefits. Composite materials produced from metal layers with different physical properties are increasingly used in modern engineering. Laminated composite metal sheets consisting of aluminum and copper layers play an important role in the industry. They are intermediate products for the manufacturing energy sector and electronics of electricity connectors, tapes, and other electric and heating conductive elements [1-3]. The advantages of these composites are a good electrical and thermal conductivity with reduced weight. Using the aluminum layer in the structure of bimetal, instead of the whole volume of copper, reduces total material costs on account of lower market price of aluminum. If a copper layer and aluminum substrate are connected to each other directly, without an Al/Cu bimetal transition piece, the service life of the electrical connection is about 1 year, but by using Al/Cu bimetal the service life is increased to more than 10 years [4].

If two layers welded together by fusion- welding method, such as laser cladding method, the formed bonds are not comparable with non-fusion welding. There is not any work published about fabrication of this bimetal by fusion-welding method. For example, M. Abbasi et al. [4] fabricated this bimetal by using cold roll welding process; M Sedighi [5] used explosive welding method and A. Khosravifard [6] used extrusion method for fabricating this bimetal. As mentioned above, these works were mainly concentrating on non-fusion welding methods and in this paper, fabrication of the first Al/Cu bimetal that produced by laser cladding method will be discussed.

Since the development of high-power lasers in late 1970s, researchers had been very successful in fabricating many new alloyed surfaces with improved wear-resistant and corrosion resistant properties [7]. The main difference between the laser surfaces alloying and laser cladding, is that the laser cladding involves significant mixing of the coating material with the substrate to form a surface layer with different phases and compositions, whereas in the alloy surface, there is not any mixing of substrate. Although, for laser cladding, mixing of the coating materials with the substrate mainly occurs at the interface and above the interface were the composition of the clad material is maintained. The surface layer created by the laser cladding is generally much thicker than that obtained by the laser surface alloying. The laser cladding in general produces 0.5–5mm or thicker clad layer, whereas, the new surface layer fabrication by the laser surface alloying is mostly less than 1mm [8].

Laser surface modification processes, including the laser hardening, laser surface alloying, laser cladding, laser annealing and laser ablation have extensively used to improve the wear and corrosion resistance of mechanical components. Alloys with superior wear and corrosion resistant properties are deposited on the surface of a substrate by coaxial powder feeding or by pre-placement of the alloy powder with subsequent laser melting, to form a thin protective clad layer. Although, direct powder feeding is a commonly used powder deposition method, the laser cladding with preplaced powder is the simplest method in depositing clad powder. In preplace laser cladding method, the powder is blended with a binder to form a paste and is brought to the surface to be cladded. In this method, it is necessary to prevent the powder particles on the substrate from removing due to the gas flow during the melting in the second step of the process [8]. To overcome this problem, the powder is usually mixed with a chemical binder to ensure its cohesion with the substrate during the process. The side effect of a chemical binder is porosity in the clad due to its evaporation during the process. In the second step of the process the following phenomena occur [8]:

1. Creation of a melt pool in the top surface of the pre-placed powder due to the radiation of laser beam
2. Expansion of melt pool to the interface with the substrate due to the heat conduction
3. Penetration of heat to the substrate causing a fusion bond

In this method, minimal dilution effects were observed for a wide range of process parameters due to the thermal barrier effect of the powder paste layer on the substrate. Laser cladding with a preplaced layer yields a thinner surface layer that typically has a thickness of more than 1 mm, resulting in low dilution with the substrate metal. In addition, cladding with preplaced powder is most advantageous for cladding of work- piece with complicated geometry, such as worm gear and bolt screw and for those places where direct powder feeding could be difficult or not feasible. Laser cladding with preplaced powder can be also applied to prototyping applications. Therefore, this method remains a popular and effective means of applying the coating material to the substrate.

In the preplaced powder laser cladding process, an appropriate laser beam mode, precise tuning of the focal point position and the optimal cladding parameters are some of the important factors in forming a thin clad layer with low dilution but sufficient bonding strength [9]. The beam mode determines the energy distribution. The laser power and the focal point position determine the energy intensity and spot size. The power and the scanning speed determine the heat input [9]. All of these factors are responsible for the transient temperature distribution, the shape of the melt pool and the final geometry of the laser clad layer. Analysis of the laser cladding process using finite element modeling is an efficient way to evaluate appropriate process parameters, to predict desirable cladding results, and to optimize the process.

In finite element modeling of welding and cladding processes, an appropriate laser heat source model has to be established to describe the physical conditions of the heat source and to incorporate them into the finite element model. In this work, a tailored laser heat source model that comprehensively takes the physical characteristics and focusing conditions of the laser beam into consideration was used. This model was presented by T. Seng in 2013 [9]. This heat source model is integrated in a finite element laser cladding model to simulate laser cladding using the preplaced powder layer technique [9]. The characteristics of the laser beam (such as wavelength, transverse electromagnetic mode (TEM), and spot size) and the cladding process parameters (such as beam power, scanning speed and focusing condition) are varied in the simulation and numerical computation to predict the temperature distribution and the clad bead profile. With the numerical results, it is then possible to predict appropriate range of beam characteristics and process parameters to achieve thin clad layer and low dilution for successful laser cladding on preplaced powder layer.

2 LASER HEATING FORMULATION

A general laser beam heat source that emerges from a focusing lens and is projected onto a work piece is depicted in Fig.1. This figure schematically depicts an emerging laser beam of a tailored TEM_{mn} mode from a focusing lens with focal length *f* and its projection on a work piece surface at a defocus distance *a* from the focal point. The radius of the laser spot projected on the surface of the work piece is *r_w*. The radius of the raw beam that emerges from the focusing lens (or mirror) is *r₀*. The spot radius at the focal point is *r_f*. A Cartesian coordinate system is attached to the beam axis. According to model of tailored laser heat source that presented by T. Seng, *q_w(r)* is obtained from Eq. 1 [9]:

$$q_w(r) = \left(\frac{r_0}{r_w}\right)^2 q_0(r) \tag{1}$$

The radius of the beam on the work piece *r_w* in Eq. (1) at any arbitrary position that is “*a*” from the focal point is approximately expressed with a linear proportional relationship as [9]:

$$r_w = \frac{f r_f + a(r_0 - r_f)}{f} \tag{2}$$

The heat flux at a radius *r* from the source Centre is [9]:

$$q_0(r) = \frac{3Q_0}{\pi r_0^2} \exp\left(\frac{-3r^2}{r_0^2}\right) \tag{3}$$

Absorption of laser power by the substrate is related to the laser-solid interaction. When an electromagnetic wave interacts with the atoms in the surface of a substrate, the field causes an electrical current. The Joule effect increases the surface temperature of the substrate due to the finite

electrical conductivity of the material [10]. Generally, the power of the laser beam is subdivided into the reflected part, the absorbed part and the transmitted part. For metals that are not transparent, the last part can be neglected [11]. The ratio between the electrical and thermal conductivity is constant and it is valid for metals, metals with good conductivity that exhibit poor absorption of laser [8].

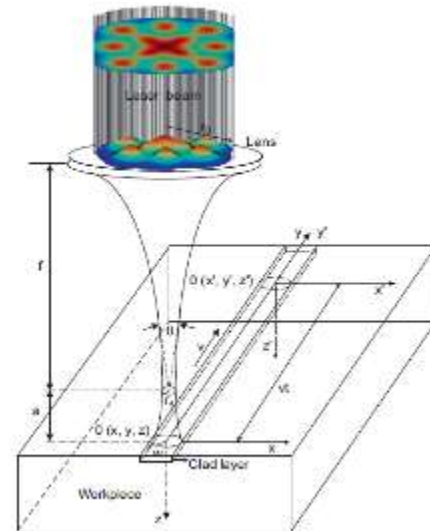


Fig. 1 Schematic illustration of the defocused moving laser heat source model of a tailored TEM_{mn} mode combining with the work piece during laser cladding [9]

Similarly, the absorption ratio (fraction of the incident laser energy absorbed by the metal surface) increases with increasing temperature because the conductivity of metals decreases. When the surface is heated continuously by a laser, the surface layers start melting which makes the electrical conductivity lower and makes the absorption ratio higher. In electromagnetic fields, the frequency affects the electrical conductivity and hence the laser light with different wavelengths shows different absorption values for a given material.

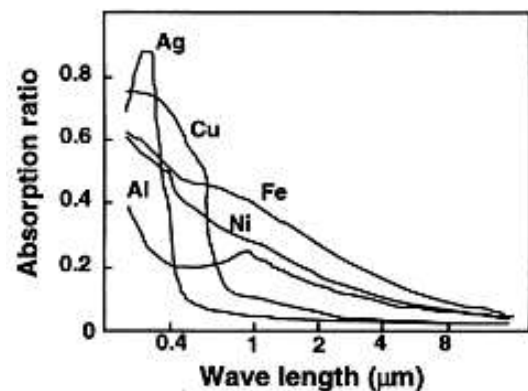


Fig. 2 Change in absorption ratio as a function of wavelength for metal surfaces [8]

Fig. 2 shows the change in absorption ratio as a function of laser wavelength for metal surface. It is recognized that the CO₂ laser with a 10.6 μm wavelength has an inferior absorption ratio to Nd:YAG laser with shorter wavelength (1.06 μm). Additionally reactions with the molten metal and the surrounding atmosphere may also affect the absorption ratio. The passing of an Nd:YAG laser beam ($\lambda=1.063 \text{ mm}$) through a focusing lens with a focal length of 120 mm and raw beam radius of 19 mm, yielded a minimal spot size at the focal point. The laser beam was defocused by adjusting the focal point at various positions above the surface of the work piece, and the radius of the defocused spot on the work piece changed accordingly. The laser power was varied from 1100W to 1200W.

Fig. 3 gives relationship between the heat flux intensity at the work piece surface (q_w) for different position of lens above the surface (a) and different laser power (P), also shows by increasing of distance position of lens from the surface, the heat flux intensity decreases. When the position of lens increased from 10 mm to 20 mm, the heat flux intensity is suddenly reduced.

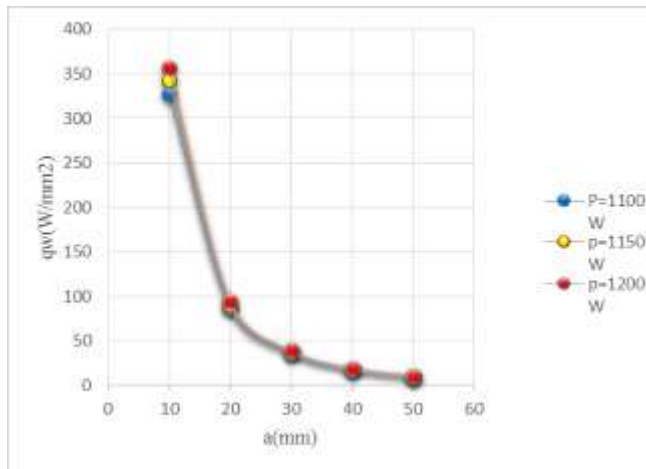


Fig. 3 Change of heat flux intensity at the different distance position of lens

3 MODELING OF LASER CLADDING PROCESS

In order to know the relationships between the laser powers, the temperature field and the heat affected zone of the cladded layer, laser heat source was incorporated in the ANSYS software. In this software, an aluminium plates (UNS A91050) were selected as substrate material and copper alloy powder (UNS C11000) was used as a clad layer material [12]. The composition and properties of Al plates and Cu powder are summarized in Table 1.

The scanning speed of laser selected 180 mm/min. In the cladding process discussed in this paper, the laser beam nozzle must rotate. In other words, due to transparent of the surface metal, the laser beam shouldn't be delivered to the surface at 90°, because the reflected laser beam from the

transparent surface of material damage the laser lens. So the laser beam was at 60° to the surface to be cladded.

Table 1 specification of aluminum and copper materials used in this investigation [12]

Cu and Al grade	Chemical composition (Wt %)	Hardness Hv3Kgf	Resistivity $\Omega \text{ mm}^2/\text{m}$
Cu-UNS C11000	99.95% Cu	45	0.0165
Al-UNS A91050	99.5% Al Max 0.25% Si Max 0.05% Mg	40	0.0276

Single-pass laser cladding of a preplaced copper powder layer on a rectangular aluminum plate was analysed using a finite element model with dimensions of 100 mm (L) \times 100 mm (W) \times 12 mm (H), as shown in Fig. 4(a). The powder layer on the substrate surface had dimensions of 50mm (L) \times 4mm (W) \times 2mm (T). The model was meshed into 25334 elements and 27662 nodes. Fig. 4(b) and 4(c) shows detail of substrate and preplaced powder layer mesh. In practice, the substrate was fixed on the work bench, so the substrate model was constrained in the z-direction.

To consider the boundary conditions, including those associated with radiation and convection, on the surface of the work piece, a surface layer consisting of three-dimensional elements with zero thickness was attached to the three-dimensional model with an identical mesh pattern to ensure nodal continuity. A small amount of heat is lost by natural convection and radiation from the surface layer. Heat conduction within the work piece model, free convection and thermal radiation between the surfaces of the work piece and the surrounding air are considered in the modelling.

Fig. 4(d) shows the division of these surfaces. Laser cladding is a complex process which has a lot of process parameters and includes the heat conduction, thermal radiation, melting and solidifying of metals, the stress and deformation of cladded layer and other physics and chemistry phenomena. In order to make investigative subject clear, a model of laser cladding should be simplified, the assumptions are as follows [8]:

1. Surface of samples is flat, except cladded layer;
2. Materials are isotropic, and their densities and thermal conductivities are depended on the temperature;
3. Influence of liquid flow on the temperature field is ignored;
4. Laser energy density is Gaussian distribution.

In order to achieve a good beam quality, it is necessary to resonate the beam laser in a resonator. In the resonator, distribution of the amplitude and phases of the electromagnetic field can be reproduced due to the repeated reflections between mirrors [13].

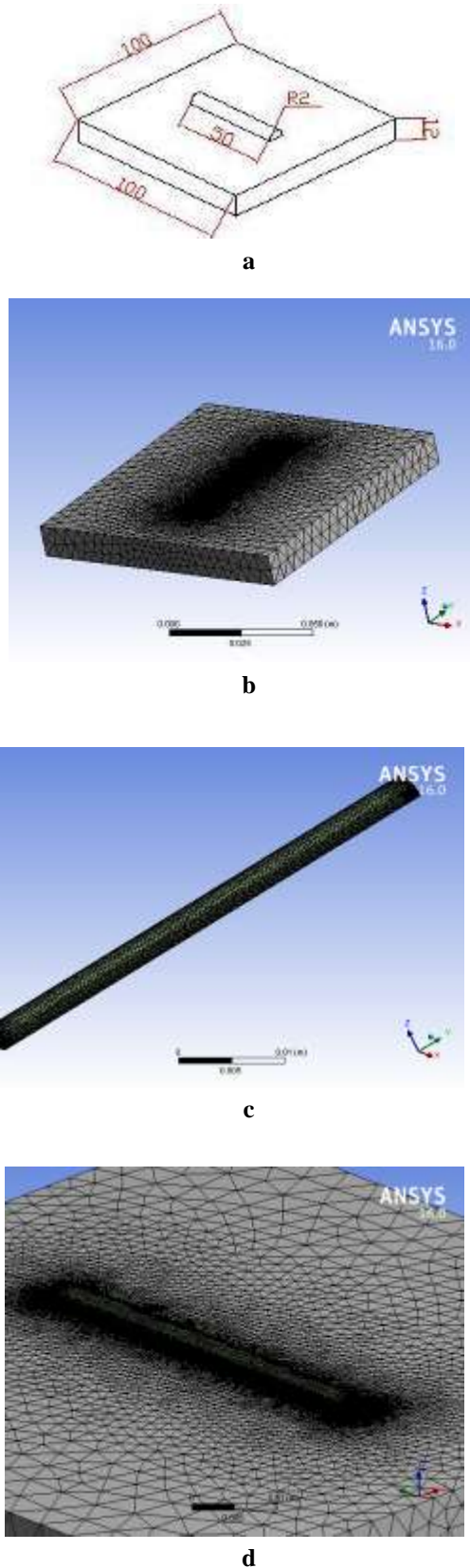


Fig. 4 Finite element modeling: (a) Pre placed powder layer and substrate, (b) Detail of substrate mesh, (c) Detail of pre placed powder layer mesh (d) division of surface for boundary condition

TEM	cross-section	distribution
TEM ₀₀		
TEM ₁₀		
TEM ₁₁		
TEM ₂₁		
TEM _{01*}		
TEM ₂₂		

Fig. 5 Several TEM modes with Gaussian energy intensity [8]

These specific field shapes produced in the resonator are known as transverse electromagnetic modes (TEM) of a passive resonator. Transverse electromagnetic modes in polar coordinates, which are also called Gaussian-Laguerre modes, are demonstrated by TEM_{mn}. The subscript m indicates the number of nodes of zero intensity transverse to the beam axis in radial direction, and the subscript n indicates the number of nodes of zero intensity transverse to the beam axis in tangential direction. Based on different TEM, various beam energy intensities are available. Fig. 5 shows several TEMs with Gaussian energy intensities. One of the important parameters for a laser beam is beam quality factor (M^2). In most cases, a laser application requires a laser beam with low divergence emitted in fundamental Gaussian mode (TEM₀₀). This is not guaranteed for every laser and is unlikely for especially high-power laser systems because the emission may be multimode or may be changed based on the life of laser systems [8].

4 NUMERICAL RESULTS

4.1 Temperature distribution and clad bead profile

To simulate laser cladding on a preplaced powder layer using the proposed laser heat source model, the TEM₀₀

mode laser beam was defocused with its focal point 10 mm above the surface of the work piece, resulting in a spot radius of 1.767 mm. The finite element model took into account thermal radiation from the upper surface and convection on the peripheral surfaces. One of the properties of the clad layer is called dilution. Dilution has two definitions: geometrical and metallurgical. The geometrical definition of dilution is illustrated in Fig. 6. According to the specified parameters in the figure, the dilution is [14]:

$$D_c = \frac{A_b}{A_b + A_c} \quad (4)$$

Where A_b is the thickness of substrate that was melted during the cladding process (mm), and A_c is the height of the clad bead (mm). In order to obtain a surface layer which is hardly diluted by the substrate material, this ratio has to be as small as possible [14]. However, if the ratio is zero, there is the risk of no fusion and bonding between cladding material and substrate. Therefore a dilution between 2% and 10% is generally accepted [14]. The dilution level depends on laser power. Using a series of experiments, van Sprang (1992) came up with an analytic expression for the amount of dilution as function of the main process parameters [15].

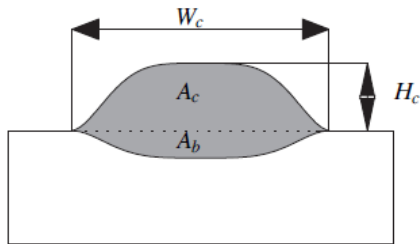


Fig. 6 Schematic cross-section of a clad layer [14]

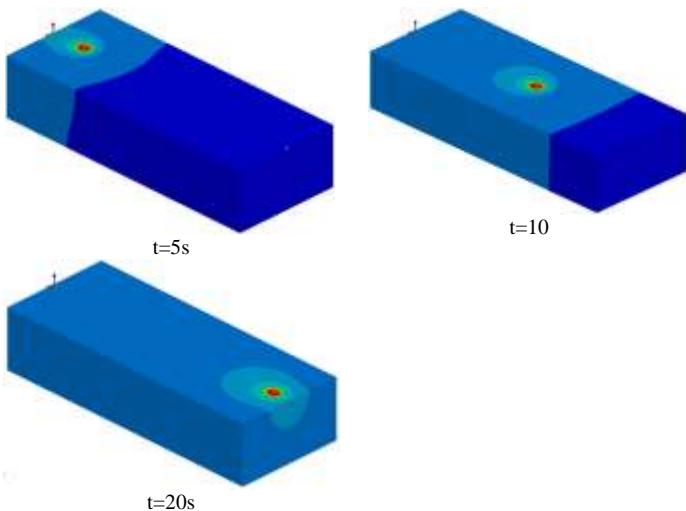


Fig. 7 Transient temperature distribution on single pas laser clad bead. Laser mode: Nd: YAG, TEM₀₀, focal point: 10mm above surface, spot radius: 1.767mm, and scanning speed: 180mm/min.

His expression shows a positive effect of the laser power, and a negative effect of both the cladding speed and clad

layer height on the amount of dilution. The profile of the melt pool reached a steady state and maintained instantaneously an unchanged profile until laser scanning completed. Fig. 7 presents the transient temperature distribution of the single pass clad bead on the work piece during Nd: YAG laser cladding at times 5s, 10s, and 20s. The clad bead profile (or the melt pool contour) is distinguished from the adjacent area by setting the temperature scale of the legends from 25°C to 1060°C. The melting temperature of the copper preplaced layer was 1045°C and the aluminum substrate melted at around 1060°C. The area where the temperature exceeds 1060°C is regarded as the melt pool.

Fig. 8 show the thermal cycles on the clad layer at $y=15$ mm, 30 mm and 60 mm along the center line of the clad bead. These thermal cycles exhibit a nearly identical peak temperature of 1060°C and a cooling rate around of 520°C/s indicate a steady state of laser cladding process.

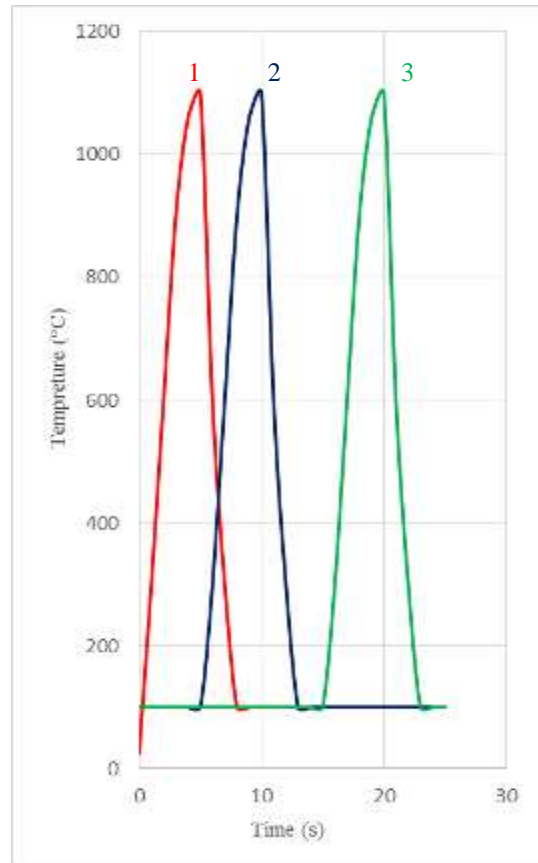
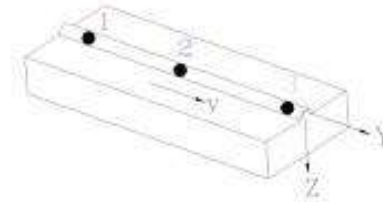


Fig. 8 Transient thermal cycles on clad bead in cladding direction

Fig. 9(a), (b) and (c) gives the relationship between the biggest depths from cladding surface under different laser powers. As can be seen from the figure, as the depth increases, the temperature decreases. Also as the laser power increased, the temperature and the depth increased. The thermal cycles and temperature profiles of the clad bead reveal a significant temperature gradient in the bead depth direction. This would result in a very limited melt depth which is desirable for laser cladding.

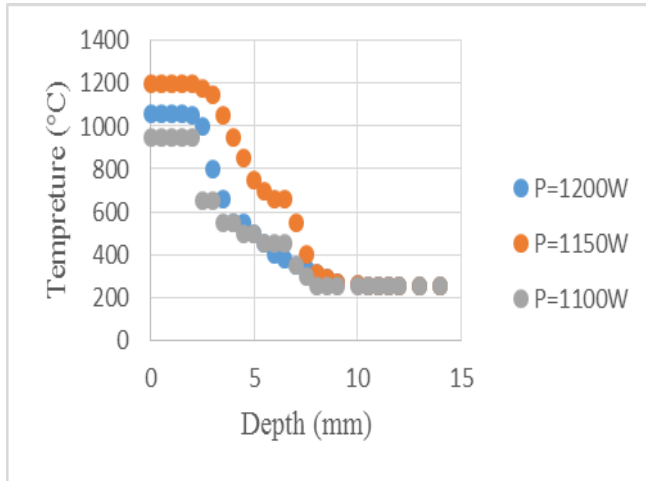


Fig. 9 Temperature profile of clad bead and substrate in thickness direction under different power laser, (a): Laser power= 1200 W, (b): Laser power= 1150W, (c): Laser power= 1100W

4.2. Laser power effect on temperature, depth and width profile of clad bead

Fig. 10 shows the laser power effect on the clad bead geometry. By applying a defocused focal point (10 mm above the surface) laser beam of a TEM₀₀ mode, both the clad bead width and depth increase with increasing laser power. The laser power exhibits a more significant influence on clad bead width than on clad bead depth, which matches the phenomena observed in the laser cladding and is desirable in a practical laser cladding process.

The laser power must exceed a threshold value so that melting of the clad layers is initiated [8]. The threshold power was determined by judging the initiation of the melting of the clad layer, so the melting temperature at 1060°C should appear on work piece during simulation. The threshold power for the initiation of melting of clad layer for Nd: YAG laser is 1150 W at which a melt pool of 1.2 mm in depth and 1.4 mm in width is reached. Also Fig. 10 depicted the transient temperature distribution profile of clad bead at t=20 s. The transverse temperature profiles clearly depict the contour of the melt pool. This figure reveals that a laser with power of 1200 W, would cause a much deeper melt pool (depth 2.4 mm, width 2.5 mm) than that of a laser with power of 1100 W and 1150 W. Deep melt pool would result in higher dilution which is undesirable for laser cladding.

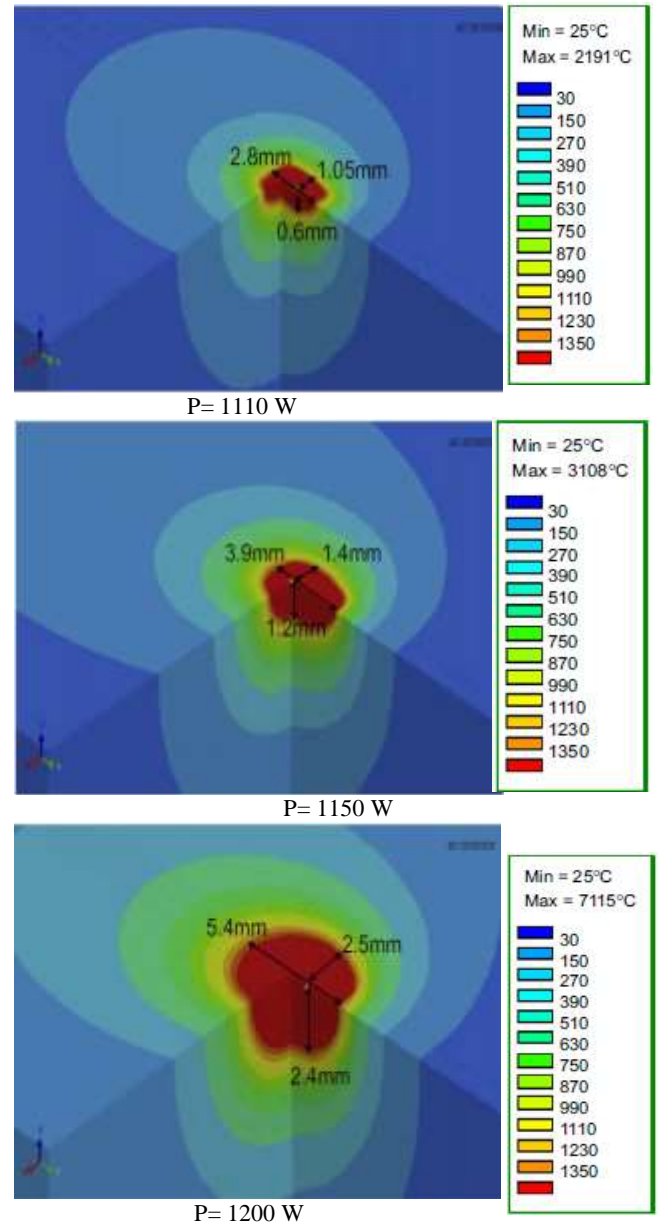


Fig. 10 Laser power effect on depth and width profile of clad bead

A laser with power of 1150 W, yield a clad bead with a reasonable profile with a depth of 1.2 mm, which is close to the desired thickness of the preplaced layer. Changing the power from 1150 W to 1200 W, increased the depth of clad bead from 1.2 mm to 2.4 mm. Fig. 9 also shows laser power effect on the width of the clad bead. A narrow width is essential for a successful laser cladding. 1200 W of laser power, yield not only an excessively large pool, but also an excessively wide width. Fig. 11 shows the relationship between laser power and depth and width of clad bead. As shown in Fig. 11, with increasing of laser power, both of depth and width increased, but it seems that the slop of depth gradient is more than the slop of width gradient, maybe the reason of this phenomenon is that the laser beam is focused to a point (Fig. 9).



Fig. 10 The relationship of laser power to depth and width

4.3. Effect of focusing conditions on geometry of clad bead

The effect of the focal point position of the Nd: YAG laser on the clad bead geometries was investigated, as shown in Fig. 12. In general, the width and depth of the clad bead decreased as the defocus distance increased. An excessive defocus distance would result in an insufficient melt depth, because with increasing of defocus distance, the heat flux intensity at the work piece surface decreased. So when a TEM₀₀ mode heat source is used, the focal point must be positioned at a distance of less than 10 mm from the surface to obtain a sufficient clad bead width of larger than 2 mm to cover the preplaced layer in the finite element model. A clad bead width of 2.4 mm was obtained from 10 mm defocus distance. The focal point should be also adjusted to ensure a complete mixing of preplaced layer with the substrate underneath, while the low dilution in the clad bead kept.

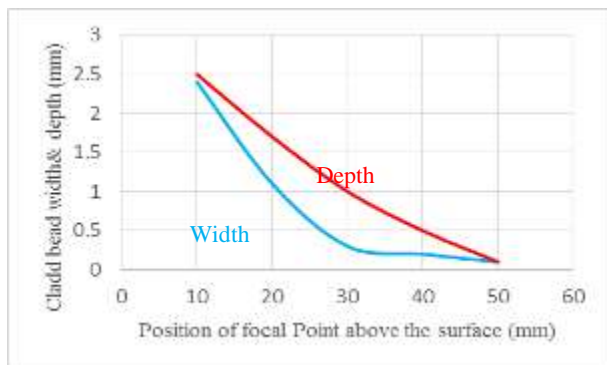


Fig. 11 Effect of focusing conditions on geometry of clad bead

5 EXPERIMENTS

5.1. Preparing of aluminum substrate and copper powder

To produce a satisfactory metallurgical bond by laser cladding method, it was essential to remove the contamination layers on of the surface of aluminium substrate. These layers are composed of oxides, absorbed ions (ions of sulphur, phosphor and oxygen), grease,

humidity and dust particles. The following treatments were performed to remove the contamination layers:

1. Rubbing surface with 240 and 320 emery;
2. Detergent washing, degreasing of surfaces, and water rinsing.
3. Final cleaning of surfaces by a powerful solvent (propanon: CH₃.CO.CH₃);
4. Scratch brushing for creating small ribs, due to formation of satisfactory bond. The bristle of the brush was made of stainless steel wire with thickness of 0.5 mm.

Copper alloy powder was used as a clad layer material that was deposited on an aluminium substrate. The powder was blended using a commercially available binder NicroBraz Cement 30-S to form a paste. The paste was pressed and then applied to the preparing aluminium substrate. When the paste dried, an approximately 2 mm thick preplaced powder layer was adhered to the substrate. Fig. 13 shows the preparing of the paste powder before laser cladding process.



Fig. 12 Preparing of paste powder

5.2. Preparing of laser welding machine

A Rofin CW025 Nd: YAG laser was used to perform single-pass laser cladding. While the Nd: YAG laser beam had a raw beam radius of 19 mm and was focused using a lens having a focal length of 120 mm to a beam radius of 0.2 mm, also defocused distance was 10 mm. The laser power for laser cladding experiment was deferent as that for the numerical model. Laser beam was improvised at 60° to the surface to be cladded. The major simulation results demonstrated in this work were obtained under a power of 1150 W and scanning speed of 180 mm/min. Argon was used as the protective gas in the experiment. The flow rate of the assist gas was 500l/h. Fig. 14 shows the laser cladding of preplace powder experiment.



Fig. 13 Laser cladding of preplaced powder

5.3. Heat treated at oven under constant temperature

After the preplaced laser cladding process, in order to investigation of influence of annealing temperature on interfacial properties of bimetal samples, the samples were

heat treated at 345°C for 1 to 10 h with temperature deviation of ± 5°C based on ASTM B917 [16].

Table 2 Regimentation of ovens

Number of oven	Annealing time (h)	Laser power (W)
1 st oven	1	1100- 1150- 1200
2 st oven	5	1100- 1150- 1200
3 st oven	10	1100- 1150- 1200

Three oven used for heat treated. In table 3, regimentation of ovens exhibits, then the interface of Al and Cu was studied by optical and electron microscopes to measure the thickness and EDX analysis to detect the composition of intermetallic compounds. Thicknesses of intermetallic layer were measured by the computer controlled image analyser of electron microscope with the precision of 0.1 micron.

5.4. Electrical resistance test

The electrical resistance of Al/Cu bimetal samples was measured by using a high precision micro- ohmmeter with accuracy of 0.01 micro-ohm. The micro- ohmmeter was passing a certain current (I) parallel to layer of sample and the measured the potential deference between tow point of the sample with defined distance (L) of the bimetal.

6 EXPERIMENTAL RESULTS AND DISCUSSION

6.1 The growth width of intermetallic compound

In order to study the quality of the interface bonding of laser cladding multilayers, a transverse cross section was cut from the samples. Then, it was examined under the scanning electron microscope (SEM). The SEM and EDS analysis was performed according ASTM E1251-11[17] and DIN EN 15079-07 [18] for aluminium and copper alloys. Fig. 15 shows an image of interface of aluminium and copper layers that product under deferent laser powers.

As it can be observed, in interface of all samples a wavy layer formed. It seems that is because of a high temperature due to spot beam radius which has been occurred at the interface of samples during the laser cladding process. Botros and Groves have completely explained the wavy interface and the mechanism of its formation in high velocity impact welding. Acarer and Demir have reported same phenomenon in their work. Also, Kacar and Acarer [19] showed that the bond interface of cladde metals (316L stainless steel and din-P355GH steel) have a wavy morphology. The obtained results from the interface of the laser cladding bimetal samples by the electron microscope (SEM) indicate that the formation and growth of intermetallic width increased by increasing the laser power. The gradual growth of intermetallic layers with increasing laser power is observed in SEM images.

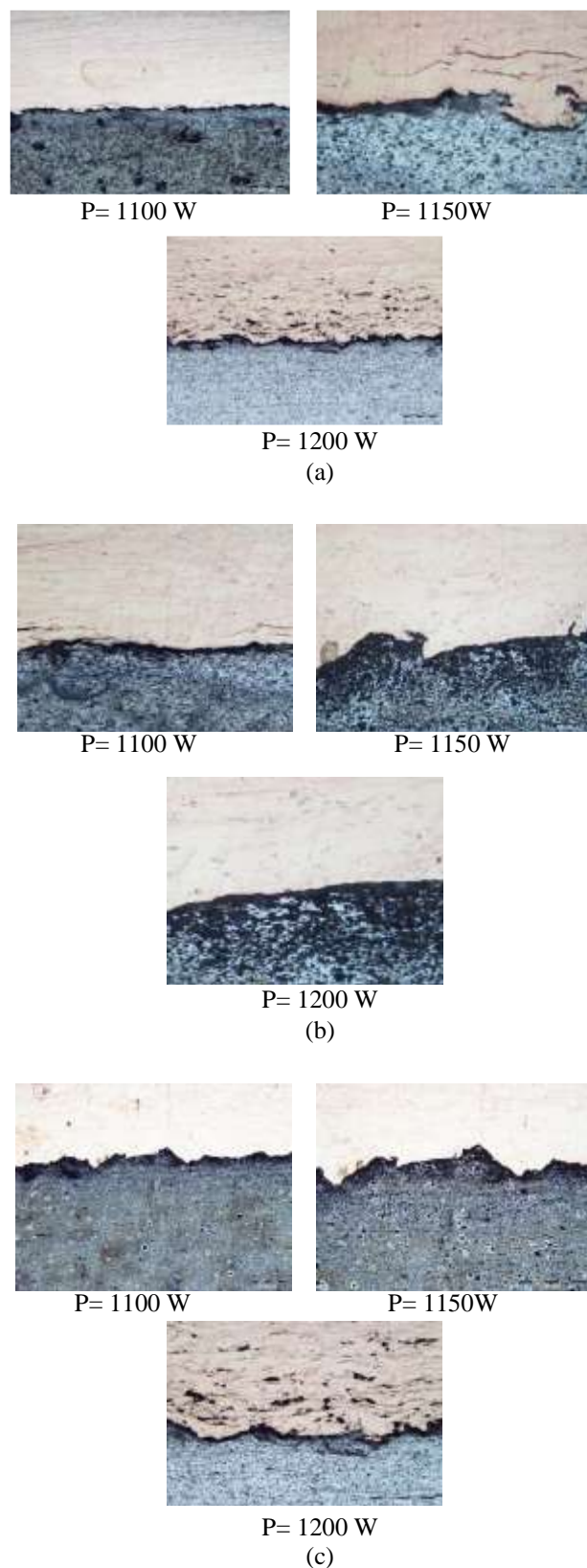


Fig. 14 The gradual growth of intermetallic layer with increasing laser power and annealing time, (a) annealing time= 1 h, (b) annealing time= 5 h, (c) annealing time= 10 h

The variation of intermetallic width (X) versus laser power (P) at constant temperature of 345° C for 10 h, in plotted in Fig. 16. From the inserted plot in Fig. 16, the relationship between laser power and the square of the intermetallic width can be presented by a linear function as below:

$$X^2 = K.P \tag{5}$$

Intermetallic width: X cm
 Growth rate: K cm²/P
 Laser power: P

K is the slope of X² versus P that is 1.2×10⁻¹⁴ cm²/w for laser power between 1100W- 1150W and 1.5×10⁻¹⁵ cm²/w for laser power between 1150W- 1200W. As can be observed, the slope of intermetallic growth between laser powers of 1100-11500 W is greater than the slope of intermetallic growth between laser powers of 11500-1200W.

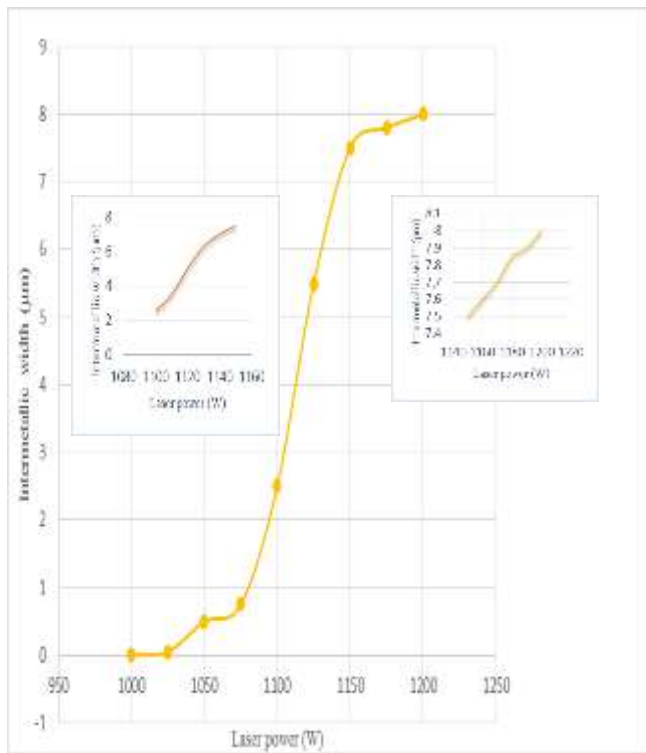


Fig. 15 Variation of intermetallic width (x) with laser power (w)

To evaluate the impact of annealing time on growth rate of intermetallic, the samples were placed in oven for 1, 5 and 10 h. Fig. 17 shows the relationship between growth of intermetallic layers with increasing annealing time for different laser power. As can be seen in Fig. 17, the width of the intermetallic compound was increased by extending the annealing time. The variation of intermetallic width (X) versus annealing time (t) at constant temperature of 345°C was measured by SEM and summarized in Table 3. The relationship between annealing time and the square of the intermetallic width can be presented by a linear function as below:

$$X^2 = K.t \tag{6}$$

K that is the slope of X² versus t that is different for different laser power presented in Table. 3. The highest value of K is 7×10⁻¹⁴ cm²/s that obtained from laser power of 1150 W and 10 h annealing time. This constant for cold roll welding and for annealing time below 1000 h is reported as 6.3 ×10⁻¹⁴ cm²/s and for friction welding under 200 h annealing time is reported as 1.6×10⁻¹³. In these works, the annealing time is greater than the annealing time in this project and it seems that the annealing time is much more effective on growth rate from welding method.

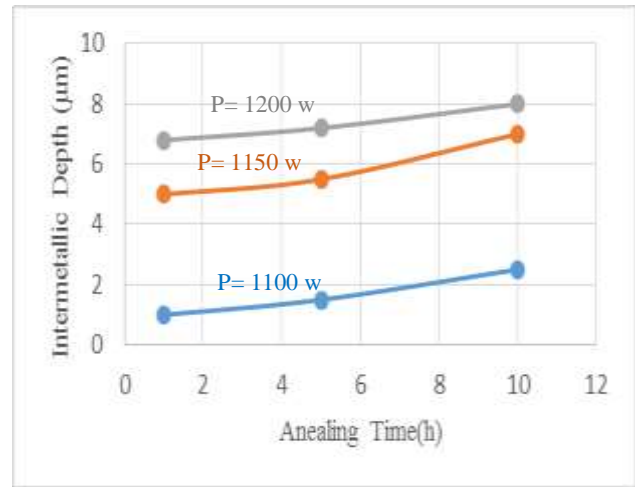


Fig. 16 Variation of intermetallic width (x) with annealing time (t)

Table 3 variation of intermetallic width with annealing time at 345°C

Times of annealing at 345°C (h)	Intermetallic layer width (µm)	Laser power (w)
1	1.35	1100
	5.21	1150
	7.01	1200
5	1.50	1100
	5.65	1150
	7.70	1200
10	2.51	1100
	7.12	1150
	8.05	1200

The highest value of intermetallic width that obtain is 8.05 µm that obtained under laser power of 1200 W and 10 h annealing time. This value is about 7 µm for laser power of 1150 W and 2 µm for laser power of 1100 W under 10 h annealing time. So according Table.3, laser power effect on growth rate of intermetallic width is greater than annealing time.

6.2 Growth rate of intermetallic compound

Table 4 reported the EDS quantitative analyses at points A, B, C and D of the areas that specified in Fig. 18. Based on this analysis, in the most important area (C), there is 73.4% Cu and 26.1% Al.

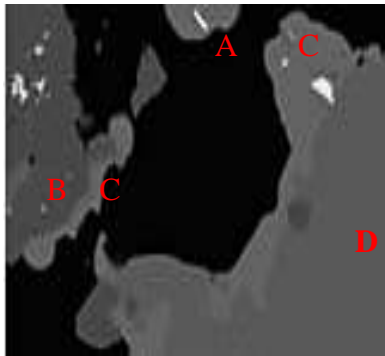


Fig. 18 EDS analysis is performed at points A, B, C and D to specify the composition of intermetallic compound

Table 4 EDS quantitative analysis at points A, B, C, D to specify the composition on intermetallic compound

	Al (at. %)	Cu (at. %)
Point A	99.5	0
Point B	97.7	1.8
Point C	26.1	73.4
Point D	0	99.9

Fig. 19 and Fig. 20 shows the percent of intermetallic compound that obtained from cold roll welding and explosive welding methods. As it can be observed, although the annealing time in these methods are very higher than annealing time in this method, nevertheless, in the most important area, percent of copper in aluminum is more than any other methods.

EDS quantitative analysis at points A, B, C, L, M

Analysis point	Atomic percent of Cu	Atomic percent of Al
A	99.87	<0.08
B	99.76	<0.08
C	92.72	7.12
D	70.38	29.62
E	51.94	47.47
F	39.50	59.35
G	38.92	57.52
H	36.17	53.02
I	47.69	51.3
J	55.59	44.41
K	3.41	96.3
L	1.07	98.32
M	0.06	95.43

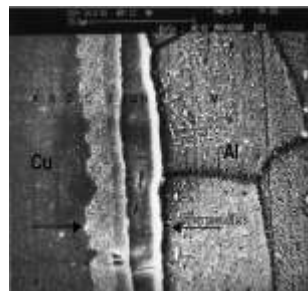


Fig. 17 Composition of each intermetallic compound in cold roll welding process [4]

EDS quantitative analyses at points A, B, C, D and E intermetallic compound.

	Al (at.%)	Cu (at.%)
Point A	0	100
Point B	30.02	69.89
Point C	52.47	47.51
Point D	69.57	30.34
Point E	99.78	0.22

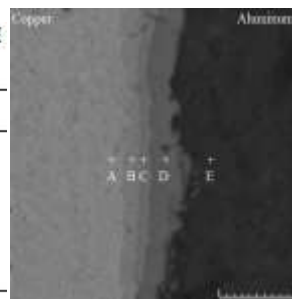


Fig. 18 Composition of each intermetallic compound in explosive welding process [5]

6.3 Resistance of bimetal samples

The results of change in resistance of the samples with increasing laser power and annealing time are presented in Table 5 and plotted in Fig. 21. As it can be observed, with increasing laser power and annealing time, resistance of bimetal reduced, because intermetallic width increased. It seems that increasing of annealing time has greater impact on reducing the resistance of bimetals.

Table 5 Resistance of bimetal samples

Annealing time at 345°C (h)	Resistance (μΩ)	Laser power (w)
1	32.83	1100
5	29.52	
10	26.74	
1	21.43	1150
5	18.62	
10	16.12	
1	20.45	1200
5	16.95	
10	15.37	

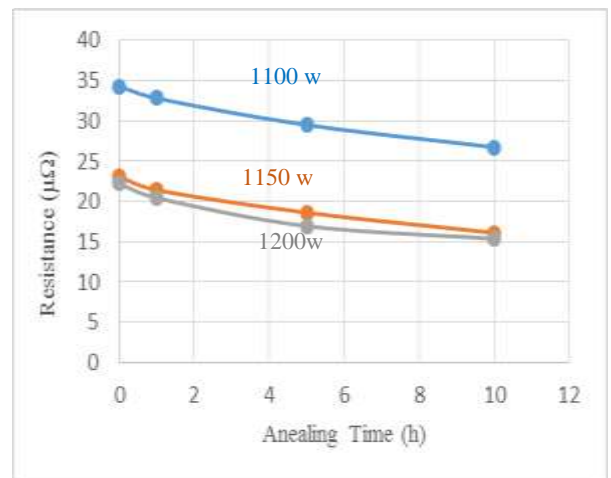


Fig. 19 Variation of resistance change with laser power and annealing time

7 CONCLUSION

In this study, laser power effect on growth rate intermetallic compounds in Al/Cu bimetals that produced by laser cladding method investigated. The following points can be concluded:

1. With increasing laser power, the size of heat effected zone increased. The heating rate and cooling rate of the cladded layer are changed by changing the laser power rapidly.
2. Examinations by the optical and the scanning electron microscopes indicate four specimens in interface of intermetallic compounds.

3. For laser cladding Al/Cu bimetal, the growth rate of intermetallic compound at a constant temperature of 345°C and for only 10 h, is noticeably greater compared with cold roll welding and explosive welding.
4. For cold roll welded Al/Cu bimetal the relation between laser power and the square of intermetallic and also annealing time and square of intermetallic can be presented by a linear equation.
5. Using such a relationship, it is possible to determine the thickness of the intermetallic layer by a non-destructive resistivity test.
6. Results of resistance of samples showed that as laser power and annealing time increased, electrical resistance of bimetals decreased.

NOMENCLATURE

Q_0	laser power at focusing lens
$q_0(r)$	the heat flux at a radius r from the source center (W/mm ²)
$q_w(r)$	the heat flux intensity at the work piece surface (W/mm ²)
r_0	laser raw beam radius at focusing lens (mm)
r_f	laser spot radius at the focal position (mm)
r_w	laser spot radius on the work piece surface (mm)
θ	beam divergence angle
f	focal length
a	distance position of lens from the surface

ACKNOWLEDGMENTS

This work was granted by Arash San'at Company under Grant Contract no 191512. Also thanks for this company for supplying materials.

REFERENCES

- [1] Mai, T.A., and A. C. Spowage. "Characterisation of dissimilar joints in laser welding of steel–kovar, copper–steel and copper–aluminium." *Materials Science and Engineering: A* 374.1 (2004): 224-233.
- [2] Eslami, P., and A. Karimi Taheri. "An investigation on diffusion bonding of aluminum to copper using equal channel angular extrusion process." *Materials letters* 65.12 (2011): 1862-1864.
- [3] Tseng, H.-C., Chinghua Hung, and Chin-Chuan Huang. "An analysis of the formability of aluminum/copper clad metals with different thicknesses by the finite element method and experiment." *The International Journal of Advanced Manufacturing Technology* 49.9-12 (2010): 1029-1036.
- [4] Abbasi, M., A. Karimi Taheri, and M. T. Salehi. "Growth rate of intermetallic compounds in Al/Cu bimetal produced by cold roll welding process." *Journal of Alloys and Compounds* 319.1 (2001): 233-241.
- [5] Asemabadi, M., M. Sedighi, and M. Honarpisheh. "Investigation of cold rolling influence on the mechanical properties of explosive-welded Al/Cu bimetal." *Materials Science and Engineering: A* 558 (2012): 144-149.
- [6] Khosravifard, A., and R. Ebrahimi. "Investigation of parameters affecting interface strength in Al/Cu clad bimetal rod extrusion process." *Materials & Design* 31.1 (2010): 493-499.
- [7] Man, H.C., K. H. Leong, and K. L. Ho. "Process monitoring of powder pre-paste laser surface alloying." *Optics and Lasers in Engineering* 46.10 (2008): 739-745.
- [8] Toyserkani, E., Amir Khajepour, and Stephen F. Corbin. *Laser cladding*. CRC press, 2010.
- [9] Tseng, W.C., and J. N. Aoh. "Simulation study on laser cladding on preplaced powder layer with a tailored laser heat source." *Optics & Laser Technology* 48 (2013): 141-152.
- [10] Gäumann, M., et al. "Epitaxial laser metal forming: analysis of microstructure formation." *Materials Science and Engineering: A* 271.1 (1999): 232-241.
- [11] Fang, L., et al. "Effect of laser power on the cladding temperature field and the heat affected zone." *Journal of Iron and Steel Research, International* 18.1 (2011): 73-78.
- [12] Harper, C.A.N.Y., NY: McGraw-Hill, . *Handbook of materials for product design*. 2001.
- [13] Mokadem, S., et al. "Laser repair of superalloy single crystals with varying substrate orientations." *Metallurgical and Materials Transactions A* 38.7 (2007): 1500-1510.
- [14] Hofman, J.T., et al. "FEM modeling and experimental verification for dilution control in laser cladding." *Journal of Materials Processing Technology* 211.2 (2011): 187-196.
- [15] Schneider, M.F.L.c.w.p., effect of some machining parameters on clad properties. Universiteit Twente, 1998.
- [16] Conshohocken, W., Standard test method for analysis of aluminum and aluminum alloys by spark atomic emission spectrometry. 2011(ASTM E1251-11).
- [17] Conshohocken, W., Standard test method for analysis of aluminum and aluminum. 2011(ASTM E1251-11).
- [18] copper and copper alloys – analysis by spark source optical emission spectrometry (S-OES); 2007(DIN EN 15079-07).
- [19] Zamani, E., and Gholam Hossien Liaghat. "Explosive welding of stainless steel–carbon steel coaxial pipes." *Journal of Materials Science Vol.47.(2)*, 2012, pp. 685-695.